Yoon, U.-S., J.-K. Park, B.G. Thomas, and I.V. Samarasekera, *85th Steelmaking Conference Proceedings*, ISS-AIME, Warrendale, PA, 2002, pp. 245-257.

MOLD CRACK FORMATION OF THE FUNNEL SHAPED MOLD DURING THIN SLAB CASTING

U-Sok Yoon[1], Joong Kil Park[2], Brian G. Thomas[3] and Indira Samarasekera[4]
[1]POSCO, Steelmaking Research Group, Technical Research Lab., Pohang, Kyungbuk, Korea, usyoon@posco.co.kr
[2]Graduate Student at University of British Columbia, 111-2355 East Mall, Vancouver, BC, Canada
[3]Department of Mechanical and Industrial Engineering, University of Illinois at Urbana-Champain, 1206 W Green Street, Urbana,IL,61801,USA
[4]Department of Metals and Metallurgical Engineering, University of British Columbia, 111-2355 East Mall, Vancouver, BC, Canada

Key Words : Thin Slab Casting, Copper Plate Crack, Funnel Shaped Mold

INTRODUCTION

An important recent trend in the steel industry is the development of processes for casting steel closer to the final product size. The continuous casting of thin slabs with thickness of only a few centimeters allows hot direct rolling to be performed in-line with conventional finishing mill, eliminating the need for a roughing train. This advanced continuous casting technology of thin slabs is growing in the steel industry owing to the associated savings in time, energy, and manpower. The mold is the most critical component of this process, which controls initial solidification and determines surface quality. The casting speed should be increased three or four times compared with conventional continuous casting to meet the productivity, Because the average heat flux is increased with casting speed due to thinner mold fluxes between mold and solidified shell, the heat flux near the meniscus would be increased much higher than increase of the average heat flux. The higher heat flux near the meniscus not only makes the uneven solidified shell but also copper plate cracks. In addition to the obvious loss of mold life due to remachinings, cracks are a serious quality problem. This is because meniscus cracks may locally retard cooling of the steel shell beneath them, and lead to longitudinal crack formation and other defects in the steel product. As the copper plate get thinner by mutiple remachinings, surface quality drops off due to the longitudinal surface cracks caused by higher heat flux in the mold. Despite its importance, the thermo-mechanical behavior of the mold and mold crack formation has received little attention and is not fully understood. Thus the present work was undertaken to improve understanding of the formation of mold crack.

PREVIOUS WORK

A few previous studies have investigated mold defects, including mathematical models and microstructural analysis to study mold crack occurrence[1-6]. Grill[1] investigated mold wear and reported that physical abrasion of the mold is related to the normal force, which acts against the copper faces. Wear occurs in regions of the mold where the air gap is fully closed. Won, et al[2], using a 2-dimensional coupled thermo-elasto-plastic finite element model of conventional slab casting, reported that wear increases with increasing narrow face taper. The width of the worn region decreases with increasing the carbon concentration in the steel.

Yoon, U.-S., J.-K. Park, B.G. Thomas, and I.V. Samarasekera, *85th Steelmaking Conference Proceedings*, ISS-AIME, Warrendale, PA, 2002, pp. 245-257.

H.Gravemann[3] analyzed surface cracks in copper billet casting mold coppers. These cracks are characterized by transcrystalline crack propagation. Corrosion fatigue was determined to be the cause and zinc and sulfur to be the corroding media. They also found that in a chrome plated mold, the corrosion of the copper starts under micro-cracks in the chrome layer forming the brittle intermetallic phases of beta and gamma brass and/or copper sulfide. Fracture of the brittle compounds leaves notches, which act as stress raisers. With alternating thermal stresses from thermal cycling, these notches ultimately develop into cracks that are 10mm deep.

Brimacombe et al[4] also studied mold cracks in billet molds, and found intergranular cracks combined with the presence of a Zn- and Pb- rich phase, suggesting that the copper plate may have undergone a liquid phase embrittlement when subjected to a tensile stress at very high temperature.

O'connor and Dantzig[5] computed cyclic inelastic strains in a funnel-shaped thin-slab-casting, to reach 1.75 pct in a region below the meniscus along the funnel edge. These large strains resulted from the combination of locally high temperatures coupled with geometric constraint of the mold. Longitudinal fatigue cracks on the hot face were attributed to over-constraint of the copper plates. They suggested cracks could be avoided by loosening the tension bolts connecting the mold with the water jacket, in order to allow the mold to move freely parallel to the broad face. They also predicted the cycles to failure for molds. Important, but complicated phenomena, such as the effect of the water box partial constraint were not considered

Sears and Badger[6] designed a cassette funnel mold which could prevent the bow found in used copper linear plates when they are removed from a mold. They suggested thin copper linear plate which have same thickness along the funnel shaped contour. But the cause of copper plate cracks is not investigated.

Most previous research has focused on conventional casting, which has a relatively low temperature field in the mold due to the small heat flux. Despite the high level of understanding that has achieved, several questions of practical importance to mold crack formation remain to be answered. Why does a funnel mold have more cracks than a parallel mold? Why do not cracks always form at the transition area of funnel mold, where O'connor found the highest stress? What is the effect of mold alloy? How many cycles to failure does an ordinary mold have with no constraint problems? What is the relative importance of thermal cycling due to metal level fluctuation compared with SEN changes? This work aims to investigate some of these issues.

EXPERIMENTS AND CALCULATION METHOD

Temperature Measurement

A plant trial was conducted with an instrumented parallel mold for a 1260mmx70mm thin slab at 3.6m/min. The mold was Cu-Cr-Zr and 1000mm long and other relevant details are given in Table 1. In this table, the effective wall thickness is defined as the minimum distance from the water channel to the hot face, and was relatively constant on each face. Fig.1 shows the back side view of the parallel mold for the plant trial, where the mold was instrumented with seven rows of thermocouples along the centerline of the mold for both the loose and fixed broad faces. Each broad face has seven columns of thermocouples across the first two rows. Thermocouples were embedded through holes drilled in the bolts to a depth of approximately 22mm from the hot face. It is noted that to prevent the mold temperature from increasing too high near the meniscus, extra angled water slots were added. The thermocouple was K type and tip of thermocouple was sharpened to reduce response time as shown in figure 2.

Yoon, U.-S., J.-K. Park, B.G. Thomas, and I.V. Samarasekera, *85th Steelmaking Conference Proceedings*, ISS-AIME, Warrendale, PA, 2002, pp. 245-257.

Table 1 Conditions for plant trial measurements of mold temperature, etc

Items	Parallel and Funnel mold
Mold coppers	Cr-Zr
Slab thickness(mm)	75
Slab width(mm)	1260
Steel grade(Carbon content, wt%)	0.04
Mold powder	
- Basicity	1.32
- Viscosity at 1300 °C(poise)	0.52
Meniscus level(mm)	100
Copper plate thickness(wide face) (mm)	60 60-85
Effective wall thickness (mm)	
- wide face	25 25-27
- narrow face	22
Mold coating material(thickness)	Cr(0.01mm)
Cooling water velocity(m/s)	
- wide face	10.7 10.5
- narrow face	10.6
Cooling water rate(l/min)	
- wide face	4330 4600
- narrow face	250
Cooling water temperature(°C)	
- inlet	37.8 39.7
- outlet	48.1 47.5
Casting speed(m/min)	3.6 4.2
Number of thermocouples(EA)	42(Fig.1) 7

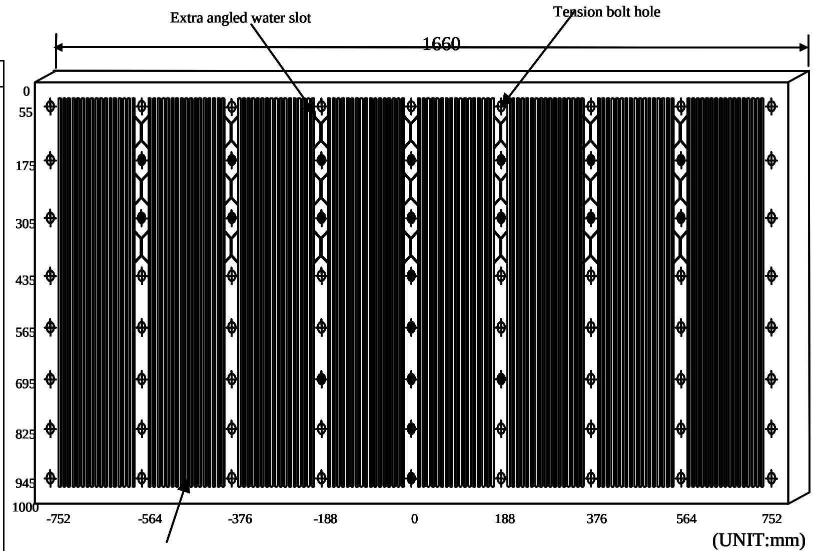

Fig.1 Back view of wide face of parallel mold showing slot geometry and thermocouple locations in bolt hole(solid circle).

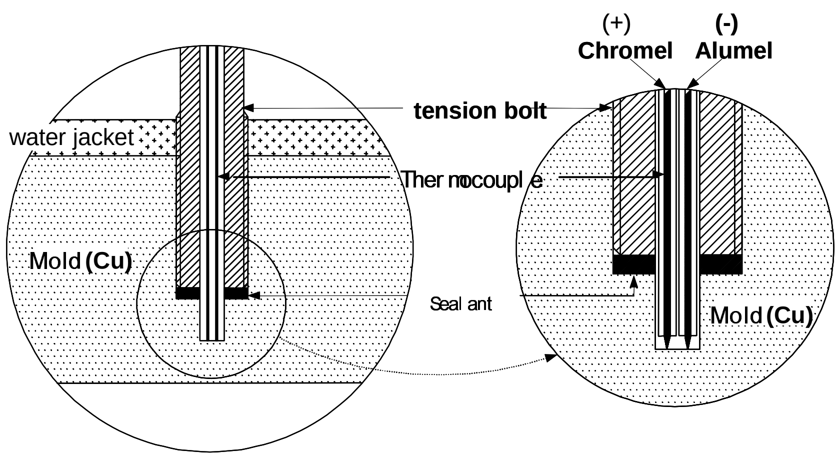

Fig. 2 Thermocouple for measuring copper plate temperature.

Temperatures were also measured in a funnel mold using similar thermocouple just at the meniscus. Attention was focused on the row of 7 thermocouples near the meniscus, 100mm below the top of the loose face of the mold, to investigate the temperature profile and thermal fluctuation in the mold and its effect on mold crack occurrence.

Yoon, U.-S., J.-K. Park, B.G. Thomas, and I.V. Samarasekera, *85th Steelmaking Conference Proceedings*, ISS-AIME, Warrendale, PA, 2002, pp. 245-257.

Other measurements

During the plant trial, various other process parameters, such as the casting speed, the metal level signal (cobalt source method), the temperature and flow rate of the cooling water were collected directly from the plant control system once per second during casting.

The temperature of the inlet and outlet of the cooling water was measured in the parallel mold. Together with the water flow rate, this temperature difference (ΔT) was used to calculate the total heat removal rate. The ΔT stayed relatively constant during the entire heat (10^{o}C), although the inlet temperatures varied from 25^{o}C to 40^{o}C on the loosed face of mold.

Mold deformation during steady state of casting was measured at the junction between the wide and narrow face of parallel mold. During assembly, the wide face of the mold contacts continuously along the narrow face edges. During operation, however, formation of a gap between these two faces above the meniscus has been reported [7]. This gap was measured using a simple metal strip gauge during steady state of casting. After casting, the mold experiences permanent deformation due to residual inelastic strain[7]. Contraction of the mold width was measured at the top of funnel mold using a ruler after 350 heats of casting.

Characteristics of copper plate cracks

The characteristics of copper plate cracks shown in figure 3 are as follows;

- The cracks are occurred longitudinal direction and frequently for funnel type mold and rarely occurred for parallel type mold.
- The cracks are occurred after first sequence operation and sometimes after several sequences.
- The cracks are located below 10~30mm from meniscus and apart 380~400mm from mold center where transition region from funnel to parallel part and coincided with tension bolt column region.
.

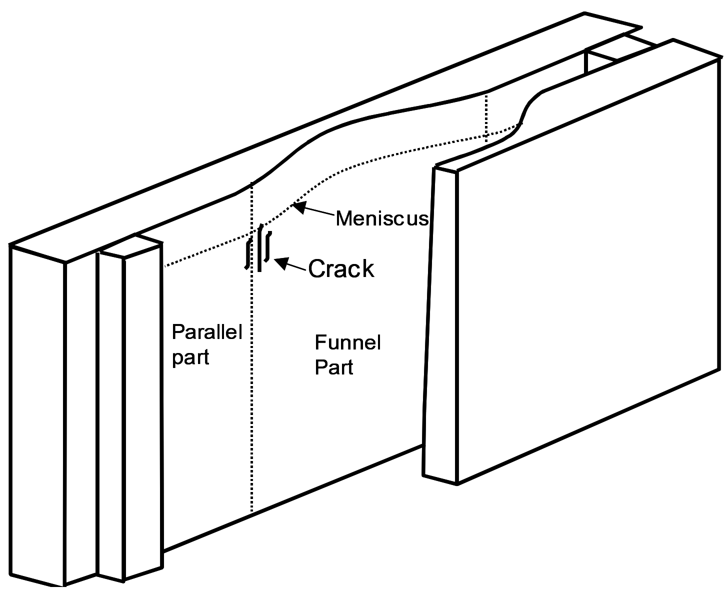

Fig. 3 Schematic drawing of the funnel mold showing location of copper plate crack.

Thermal stress computational model description

Two dimensional (2-D) finite-element models are applied to calculate temperature and the corresponding stress and strain filed in the parallel and funnel mold using commercial stress-analysis package, ABAQUS 5.8[8]. Simulation conditions are given in Table 1. Horizontal sections of one-quarter of the mold (2-D quarter model), including part of the water jacket were taken at the height corresponding to the highest mold temperature, as shown in Fig.4. These slice sections were assumed to deform in plane strain. This section is reasonable because the surface cracks were always longitudinal along the mold length. To obtain accurate predictions from a 2-D model of a 3-D phenomena, special boundary conditions were developed in order to match the 3-D model predictions. First, heat flux boundary condition at hot face of the 2-D quarter model were chosen lower than physically measured in order to match the temperature predictions of the full 3-D segment model. To obtain stress model boundary conditions, the 3-D quarter model was first run using the thermal load to reproduce 50 thermal cycles experienced in real the mold. Symmetry planes at the wide-face centers are mechanically constrained to prevent normal displacements. To realize the pre-tension force into 2-D quarter model, the u and v displacements of the backing plate at each tension-bolt position from 3-D analysis (3-D quarter model) were imposed as fixed-displacement boundary conditions on each tension bolt position in the 2-D quarter model.

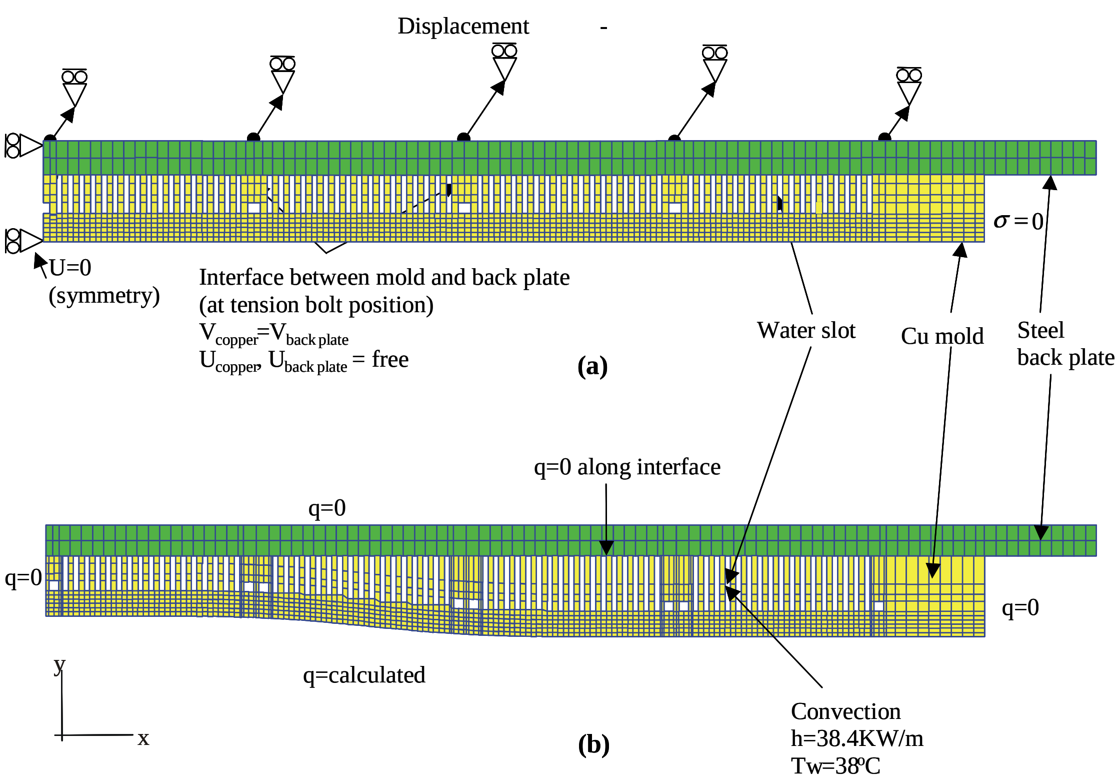

Fig. 4 Finite element mesh of 2-D horizontal domain for parallel and funnel mold and its thermal and mechanical boundary conditions.
(a) Parallel mold and stress B.C (b) Funnel mold and heat B.C.

The heat flow model solves the transient heat conduction equation[9] for the temperature distribution in the various model domains. Heat flux data was chosen to input to the exposed surfaces of copper elements on the mold hot faces.

A water-slot heat transfer coefficient h_1, was applied to the surface of the water slots and using the correlation of Dittus and Boelter[10].

$$\frac{h_1 D}{k_w} = 0.023\left(\frac{DV_w \rho_w}{\mu_w}\right)^{0.8}\left(\frac{Cp_w \mu_w}{k_w}\right)^{0.4} \tag{1}$$

Where, D is hydraulic diameter of slot, k_w is thermal conductivity, μ_w is viscosity, ρ_w is density, C_{pw} is specific heat of cooling water, V_w is cooling water velocity. For the cooling water channel geometry and velocities in Table 1 and 2, this produces heat transfer coefficient of 38.45kW/m^{2}K on the wide face and 36.17W/m^{2}K on the narrow face of mold.

Table 2 Simulation conditions

a) Mold geometry

Mold length(mm)	1000
Mold width(mm)	1660
Slab width(mm)	1260
Copper plate thickness(mm)	60(parallel) 80(funnel)
-wide face	75
-narrow face	35
-Water slot depth(mm)	5
Water slot thickness(mm)	4.6
Distance between slots(mm)	5X10
Nominal cooling water section(mm)	445
Bolt length(mm)	16
Bolt hole diameter in water jacket(mm)	24
Distance between bolts(mm)	188
Water box thickness(mm)	360
Clamping force(kN)	
- top(0.58m from bottom)	19
- bottom(0.1m from bottom)	44
Tension bolt force	
- tightening torque, N-m	120
- fricition coefficient	0.1

b) Material properties

Items	Copper(plate)	Steel(Bolt)
Conductivity(W/mK)	350	49
Density(Kg/m^3)	8960	7860
Specific heat(J/Kg K)	384	700
Elastic modulus(Gpa)	115	200
Thermal expansion Coeff.(1/K)	17.7X10^{-6}	11.7X10^{-6}
Poisson ration	0.34	0.3

To simulate thermal cycling of the mold over a complete campaign, it was assumed that the mold was heated from room temperature to the operating temperature by sudden immersion in the high temperature environment for 100 seconds, followed by 4 hours of steady casting for each sequence which includes 5 ladle changes. It was then cooled to room temperature, over 360 seconds after each sequence, which defines a single thermal cycle.

Heat flux profiles

To compare the thermo-mechanical behavior of parallel and funnel molds using the quarter mold model. To enable a comparison isolating the effect of geometry alone, heat flux, q, in both molds was defined by the following equations[11].

$$q(KW/m^2) = 5403 - 990\sqrt{t(\sec)} \tag{2}$$

RESULT AND DISCUSSION

Morphology of mold cracks

Photograph and micrographs of the mold cracks of interest in this study are presented in Fig. 5. Sometimes, cracks were observed after only 2 or 3 sequence of casting, but, from time to time, molds were in service with no crack for about 70 sequence. Most of the cracks formed just below the meniscus, and were located about 380mm from the center of mold, at the transition region of the funnel shape in the same location as observed by O'connor[5]. A closer examination of the mold surface around the crack reveals two distinct regions, which are identified in Fig.5. The top and bottom part of the specimen is dark gray (Fig.5 A) which corresponds to the Cr coating layer. Around the crack, which is found near the meniscus, it shows the yellow color (Fig.5 B). Its composition was identified as a brass using the energy-dispersive spectrum (EDS) on the scanning electron microscope (SEM) (Fig.6).

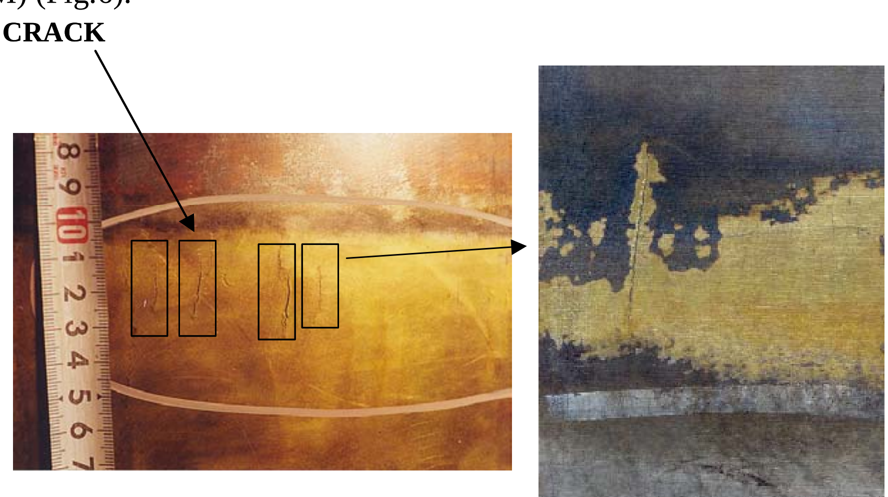

(a) (b)

Fig. 5 Photographs of (a) mold crack and (b) magnified view.

Yoon, U.-S., J.-K. Park, B.G. Thomas, and I.V. Samarasekera, *85th Steelmaking Conference Proceedings*, ISS-AIME, Warrendale, PA, 2002, pp. 245-257.

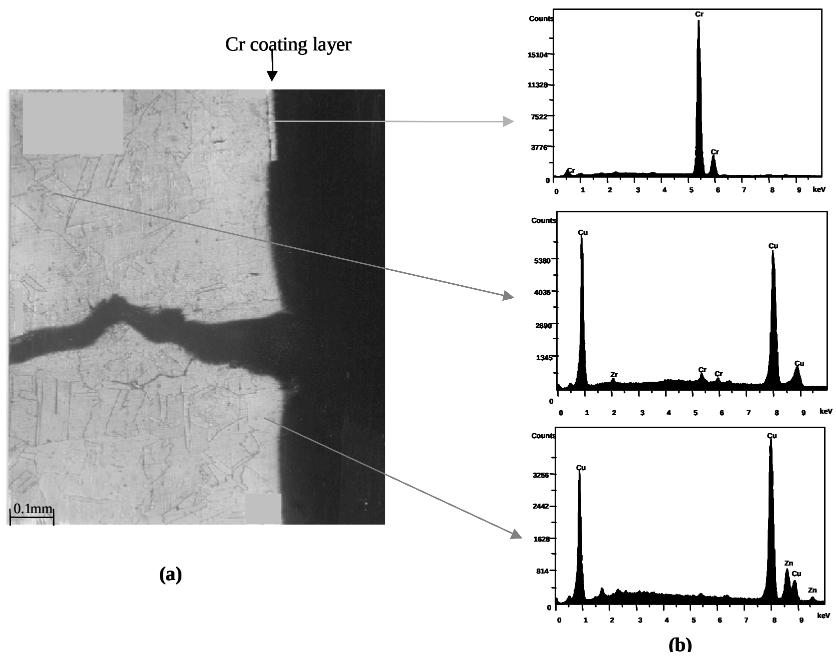

Fig. 6 Optical micrograph of (a) mold crack around the top of crack and (b) X-ray spectrum.

The striking feature of the crack occurrence is that near the top surface of the mold, the Cr plated layer is absent from around the crack as shown in Fig.6. Instead of the Cr layer, a brass layer was formed just beneath the hot face of mold, in which Zn concentration reached up to 16% from EDS analysis. The molten metal appears to be the only possible zinc source. Zinc absorption into the hottest portion of the mold surface was also reported by O'connor et al[5], but only where its temperature exceed 425^{o}C. These results suggest that the hottest portion of the hot face of the copper lost its protective Cr layer, exceeded 425 ^{o}C, was severely attacked by Zn in the molten metal, and formed brass. This alloy is relatively brittle and acted as stress raiser to initiate intergranular fracture, which propagated deeper via transgranular thermal fatigue.

Scale Deposition

Nucleate boiling at the mold/cooling water interface favors the deposition of scale if water quality is poor.[9] The deposition of scale reduce the heat transfer then causes the surface temperature to rise. Fig. 7 shows the scale at the meniscus region and its EMPA analysis for waste funnel shaped copper plate. The scale deposits severely just below the meniscus and coincided with the place where high temperature of the copper plate developed. The element of scale was Fe and this scale could cause the copper plate crack by reducing the heat transfer between copper plate and cooling water interface and then increasing copper plate temperature. Even though the scale was also found at the slot of parallel mold just below the meniscus, copper plate crack was not occurred. Scale deposition increases the copper plate temperature and can increase the thermal strain.

Yoon, U.-S., J.-K. Park, B.G. Thomas, and I.V. Samarasekera, *85th Steelmaking Conference Proceedings*, ISS-AIME, Warrendale, PA, 2002, pp. 245-257.

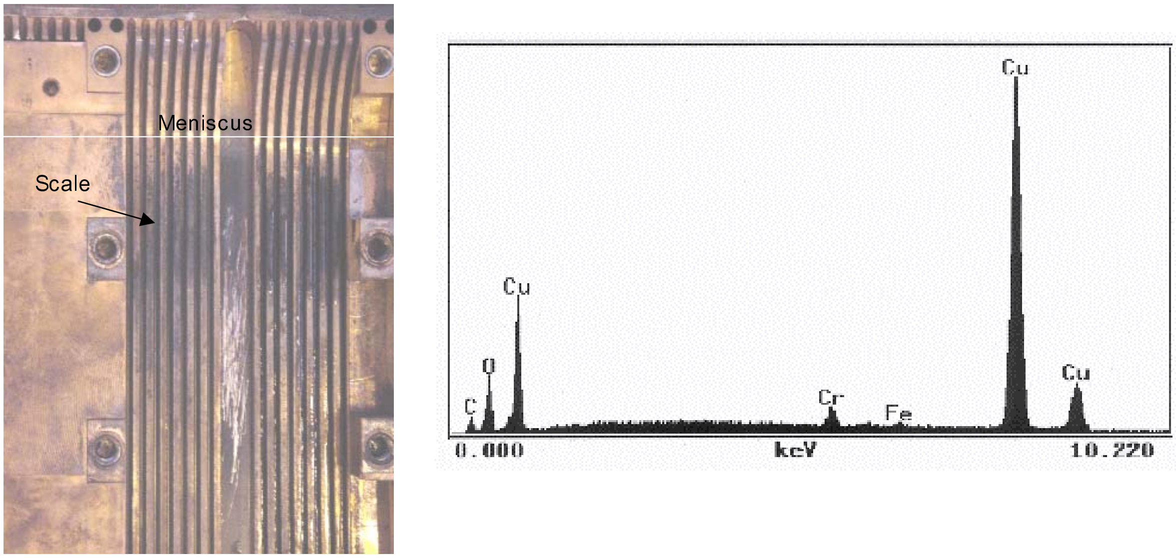

Fig. 7 Scale deposition just below the meniscus at cooling slot and its EPMA analysis.

Thermal Stress Analysis of copper plate

To isolate the effect of mold shape alone on temperature, stress, and crack occurrence, the same heat flux ($4MW/m^2$) was imposed on 2-D quarter models of the funnel and parallel molds. Fig.8 compares the temperature distributions calculated along the hot face of the two molds. As seen in this figure, the funnel mold shows a variation of temperature across the mold width despite the constant heat flux. In particular, the region around the funnel transition region where the cracks occurred regime, shows a peak in temperature of about 20°C. This phenomenon is attributed to local variations in the slot geometry for the funnel mold. As shown in Fig.9, the distance between the hot face of mold and slot root (slot-depth) is not uniform across the funnel mold width. In particular, the funnel transition region has deeper slots, ranging from 0 – 3mm further from the hot face than the others.

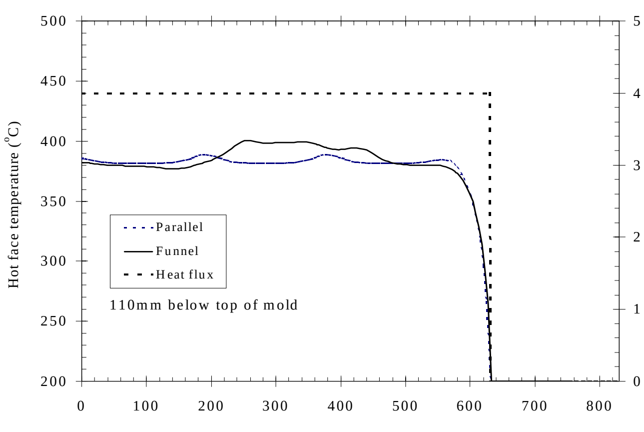

Fig. 8 Comparison of hot-face temperature distribution across the wide face with different mold shape. (2-D slice model)

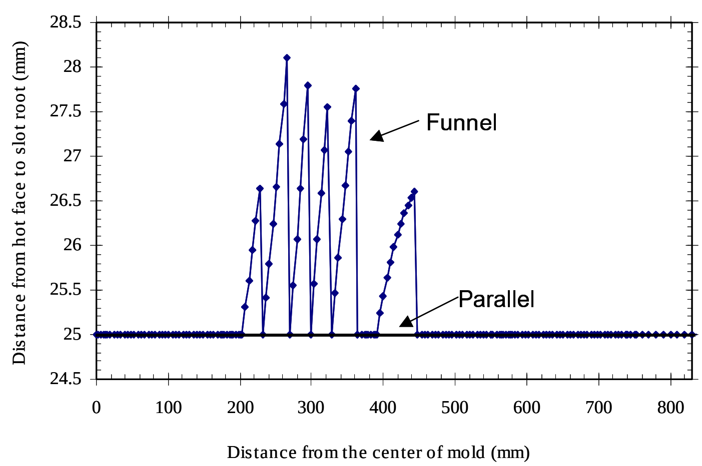

Fig. 9 Slot depth profile cross the mold width at the meniscus for the parallel and funnel mold.

This is because the slots are machined to equal depths in groups of 3 or 4 slots as shown Fig. 10.

.

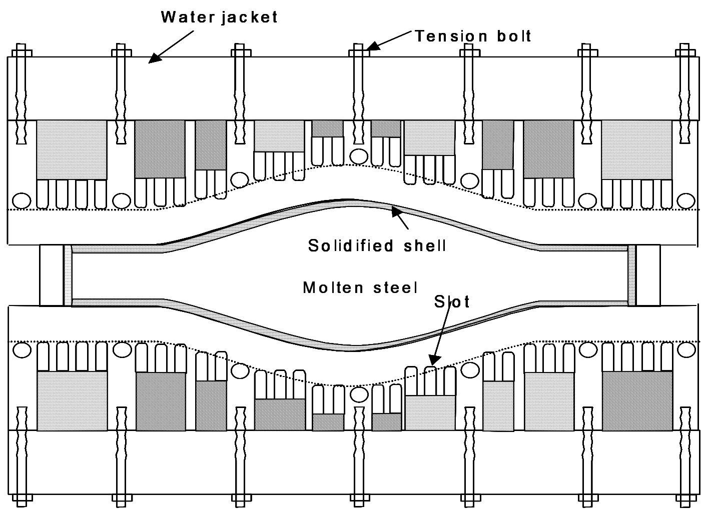

Fig. 10 Schematic drawing of funnel mold which shows the slot are machined to equal depths in a groups 3 or 4 slot for funnel curvature.

Typical stress and strain results from the 2-D quarter model are shown in Figs.11and 12. Fig.11 compares the Von Mises stress profiles across the hot face width of both molds. Fig.12 compares the inelastic strain (equivalent plastic strain plus equivalent creep strain) distributions across the hot face together the region of crack occurrence. Where the hot face temperature is higher in the funnel mold, the stress and strain results are also higher. Thus, both of these fracture criteria correctly indicate the location of cracks and suggest a relationship with the water slot array.

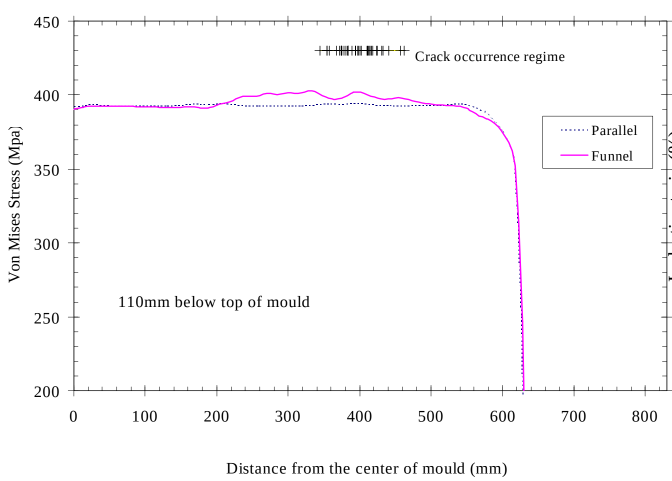

Fig. 11 Comparison of Von Mises stress across the hot face with different mold shape.

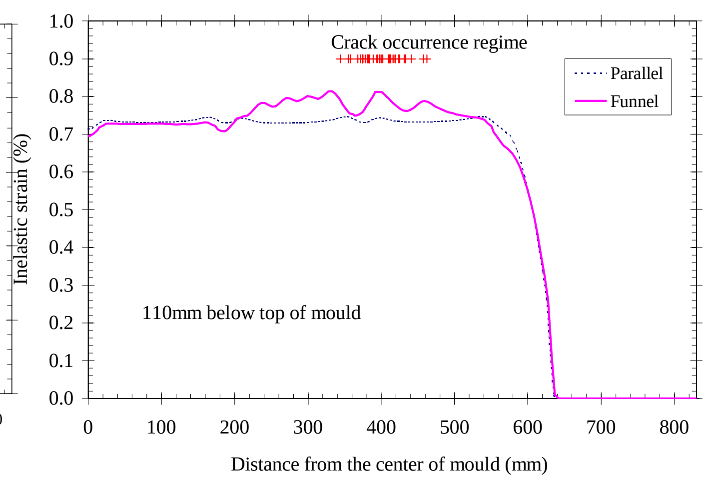

Fig. 12 Comparison of inelastic strain distribution across the hot face with different mold shape.

The magnitude of the differences in both stress and strain between the cracked and non-cracked locations is very small, however. Thus, these results explain only the location where cracks initiate in the funnel mold. They do not completely explain the difference in susceptibility between the funnel and parallel mold shapes.

To investigate the relationship between temperature profile, stress, and cracks near the meniscus, mold temperatures were measured at the meniscus in a funnel mold. Fig.13 shows the temperature response at different positions across the hot face at the meniscus during steady state casting. The temperature 376mm from the mold center is higher than other locations by 50^{o}C. This was expected due to slot variation as shown in Fig. 9.

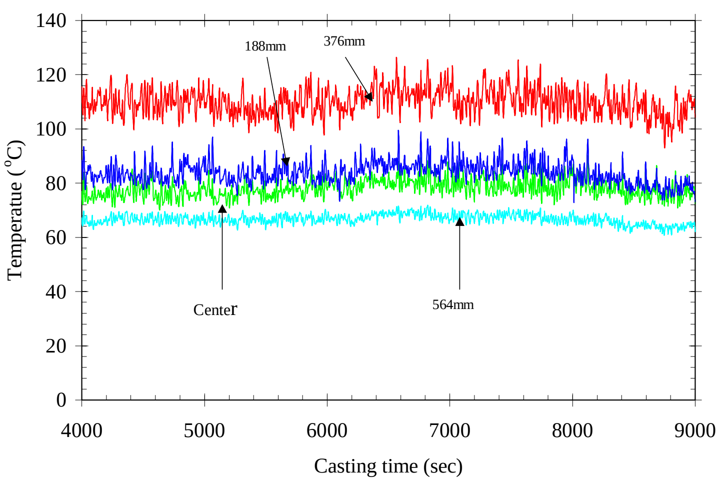

Fig. 13 Measured temperature in funnel mold at the meniscus during steady state(100mm below mold top).

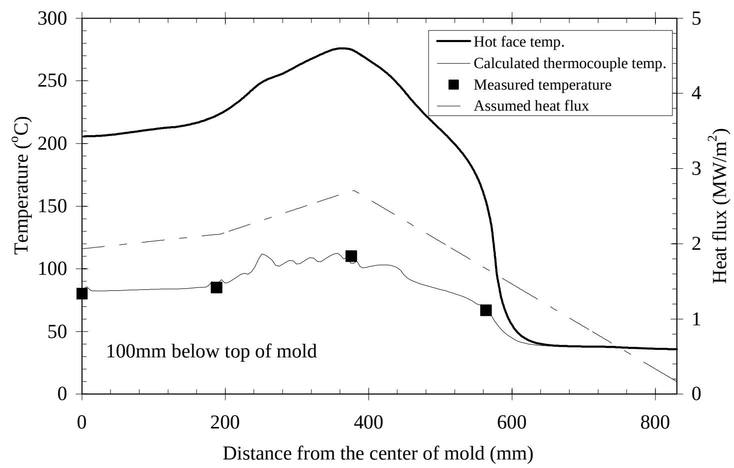

Fig. 14 Comparison of calculated temperature profile and measured ones and corresponding hot face temperature and heat flux profile across wide face at the meniscus region of funnel mold(2-D slice model).

Based on the measured temperatures, the 2-D quarter model was used to calculate temperature, stress and strain distributions. Fig.14 shows the temperature distribution across the hot face and thermocouple location, including the corresponding heat flux profile adjusted for the 2-D quarter model. It can be seen that hot face temperature variation is significantly more severe than at the thermocouple depth. The funnel transition region is more than 70^{o}C hotter than the center region of the funnel mold. O'connor[5] suggested that the outer bend of the funnel region is hotter due to convergent heat flow. Stress and plastic strain in the transverse plane follow the temperature profile, and have peak values, which coincide with the region of crack occurrence, as shown in Figs.15 and 16. These results provide even stronger evidence that the cracks initiate in the funnel transition area due to higher temperatures and stress concentration in this region.
To release the stress concentration, tension bolt near the crack occurrence region removed and tapped the bolt to prevent the leakage of cooling water as shown in Fig. 17. The service life of copper plate increased three times.

Yoon, U.-S., J.-K. Park, B.G. Thomas, and I.V. Samarasekera, *85th Steelmaking Conference Proceedings*, ISS-AIME, Warrendale, PA, 2002, pp. 245-257.

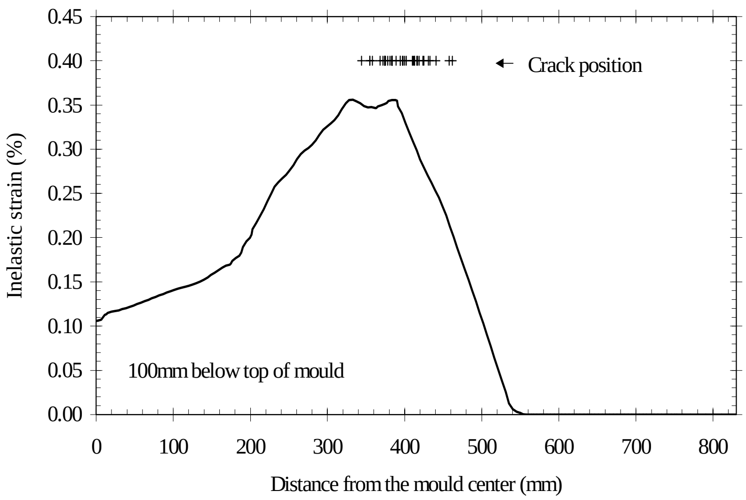

Fig. 15 Stress(σ_{xx}) profile across wide face of funnel mold.

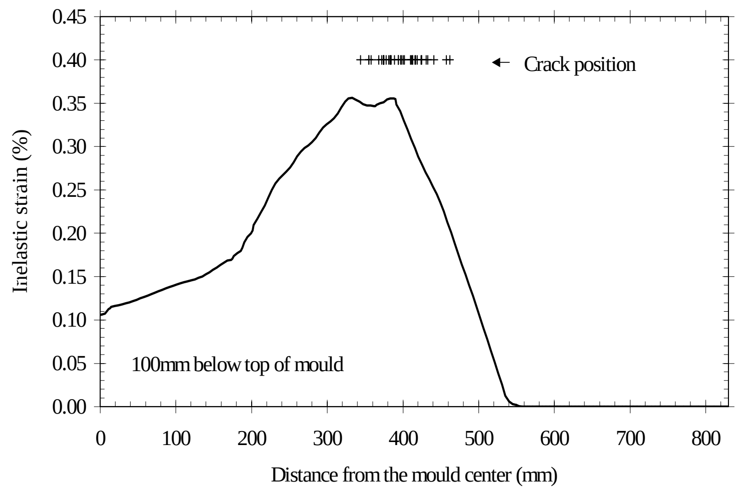

Fig. 16 Inelastic strain profile across wide face of funnel mold.

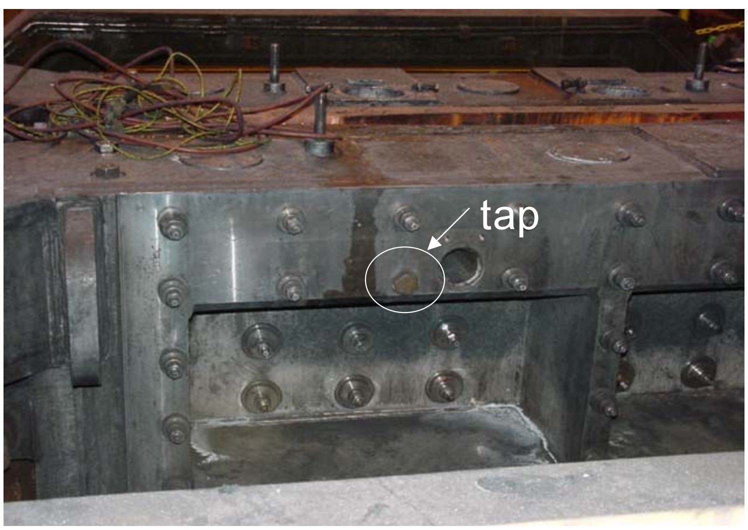

Fig. 17 Removed tension bolt at backside of water jacket for stress relief.

SUMMARY

The formation of cracks in a funnel mold for casting of thin slabs is investigated using metallographic studies and mathematical models.

1. The initiation of crack is associated with the formation of brittle compound relative to the matrix, which acts as a stress raiser for the crack initiation at the high temperature region.
2. Scale deposition at the slot just below the meniscus increased the hot face temperature of copper plate.

Yoon, U.-S., J.-K. Park, B.G. Thomas, and I.V. Samarasekera, *85th Steelmaking Conference Proceedings*, ISS-AIME, Warrendale, PA, 2002, pp. 245-257.

3. The slot depth of funnel mold has variable distance from the hot face and the range of slot-depth is 25-28mm in the funnel transition area, which results in slightly higher stress and strain fields relative to parallel mold.
4. By removing the tension bolt near the crack occurrence region, service life of copper plate increased 3 times and this means stress concentration is main cause of copper plate cracks.

ACKNOWLEDGEMENTS

The authors would like to thanks all co-authors for their contribution to this work. Special thanks to Chulmin Kim of Thin Plate Team of minimill, POSCO and Mr. Neil Walker for technical support.

REFERENCES

1. A.Grill, K.Sorimachi and J.K.Brimacombe: Metall. Trans., 7B ,1976, p.177
2. Y.M.Won, T.J.Yeo, K.H.Oh, J.K.Park, J.Choi, C.H.Yim: ISIJ International, Vol.38,1998,No.1, pp.53-62.
3. H.Gravemann, J.I. Brown and C.D.Tapley*:* AIME, 1981, pp. 22-34
4. E.B.Hawbolt, F.Weinberg and J.K.Brimacombe : Continuous Casting, Vol.2, AIME, 1984, pp.85-102
5. T.G. O'connor and JA Dantzig : Metallurgical Transactions B, Vol. 25B, 1994, pp. 443-457
6. James B. Sears Jr. and Michael R. Badger: 84th Steelmaking Conference Proceedings, Vol.84(2001) p249
7. B.G. Thomas, G.Li, A.Moitra and D.Habing : Iron and Steelmaker, Oct., 1998, pp.125-143.
8. K.Hibbit and J.Sorensen, ABAQUS, Providence, RI, 1996.
9. I.V. Samarasekera, J.K.Brimacombe : Ironmaking and Steelmaking, Vol.9, No.1, 1982, pp.1-15
10. F.P.Incropera and D.P.Dewitt, "*Fundamental of Heat Transfer*", J. Wiely& Son, 1981, p.401
11. J.K.Park, B.G.Thomas, and I.V Samarasekera : 83rd Steelmaking Conference Proceedings, ISS-AIME, 2000, pp.9-21